Electronic Supplementary Material (ESI) for Analytical Methods.

A Chemodosimetric Chemosensor for the Ratiometric Detection of Nerve Agent-Mimic DCP in Solution and Vapor Phase

Shilpita Banerjee[a], Pintu Ghosh[a], Anirban Karak[a], Dipanjan Banik[a], Ajit Kumar Mahapatra[a*]

[a]*Molecular Sensor and Supramolecular Chemistry Laboratory, Department of Chemistry, Indian Institute of Engineering Science and Technology, Shibpur, Howrah 711 103, India*

*Author to whom correspondence should be addressed; electronic mail: akmahapatra@chem.iiests.ac.in; Tel.: +91 – 9434508013

*Corresponding author. Fax: +91 33 26684564; Tel: +91 33 2668 4561;
E-mail: mahapatra574@gmail.com (A. K. Mahapatra)

Table of Contents

1. Table S1 Comparison between previously reported DCP sensors with the current work

Sl. No.	Probe structure	Solvent	Binding mechanism	Response time	LOD	Application	Reference
1.	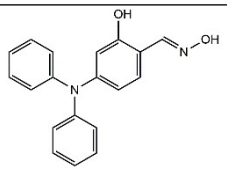	CH_3CN	Cyclization to benzisoxazole	<1 min	0.14 μM.	Vapor phase, Live cells	1
2.	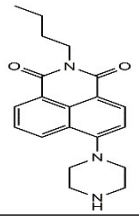	DCM	Phosphorylation at -NH	300 s	5.5 nM	Vapor phase	2
3.	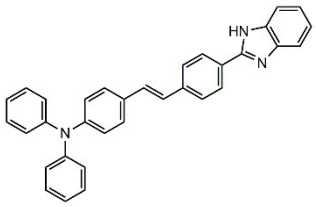	THF	Phosphorylation at -NH	40 s	8.45×10^{-8} M	Vapor phase	3
4.	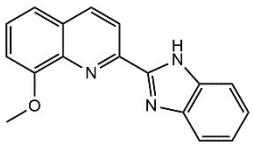	$CHCl_3$	Phosphorylation at -NH	<2 min	8.45×10^{-8} M	Vapor phase	4
5.	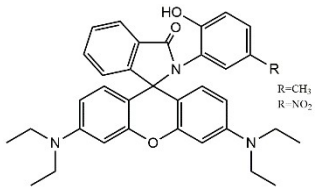	DMF	Phosphorylation followed by ring-opening	10 s	1.4 nM	Vapor phase	5
6.	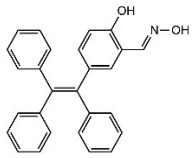	CH_3CN	Phosphorylation at -OH	3 min	0.12 μM	------	6
7.	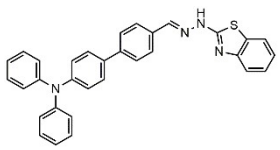	THF	hydrolysis of imine	2.5 min	3.56×10^{-8} M	Vapor phase, Live cells	7
8.	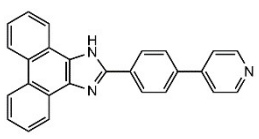	DMSO	Phosphorylation followed by hydrolysis of phosphate	18 s	1.4 nM	Vapor phase-cotton biopolymer	8
9.							9

	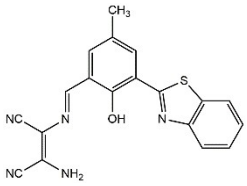	CH_3CN	deimination	28 min	0.43 µM	Vapor phase, Live cells	
10.	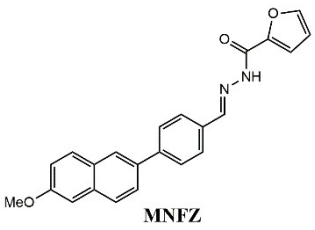 MNFZ	CH_3CN	hydrolysis of imine	100 s	12.2 nM	Vapor phase-cotton biopolymer	This work

2. Computational method

Theoretical calculations

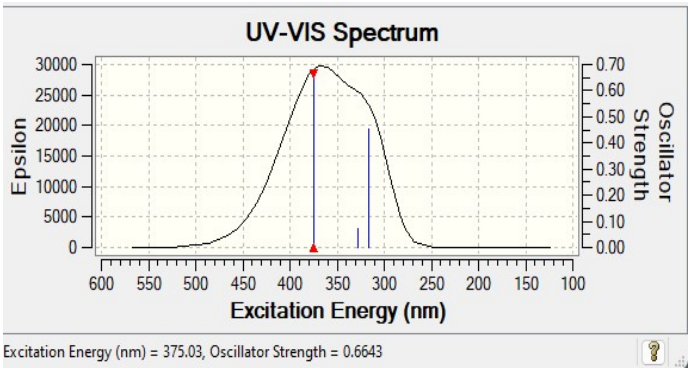

Figure S1. Absorption spectra of the Probe (**MNFZ**)

Table S2 The vertical main orbital transition of the **MNFZ** calculated by TDDFT method

Energy (eV)	**Wavelength (nm)**	**Osc. Strength (f)**	**Transition**
3.3060	375.03	0.6643	**HOMO ⟶ LUMO**
3.7844	327.62	0.0705	**HOMO ⟶ LUMO + 1**
3.9244	315.94	0.4531	**HOMO-1 ⟶ LUMO**

3. Calculation of Limit of detection

From the plot of fluorescence intensity ratio I_{528}/I_{434} vs concentration of DCP limit of detection was calculated by using the formula LOD= k ×δ/m where k= 3, δ is the standard deviation of the intensity ratio (I_{434}/I_{527}) of blank solution (0.008163) and m is the slope of the calibration curve (2.00×10^6).

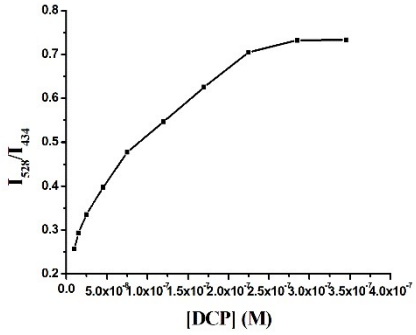

Figure S2. Plot of fluorescence intensity ratio vs concentration of DCP

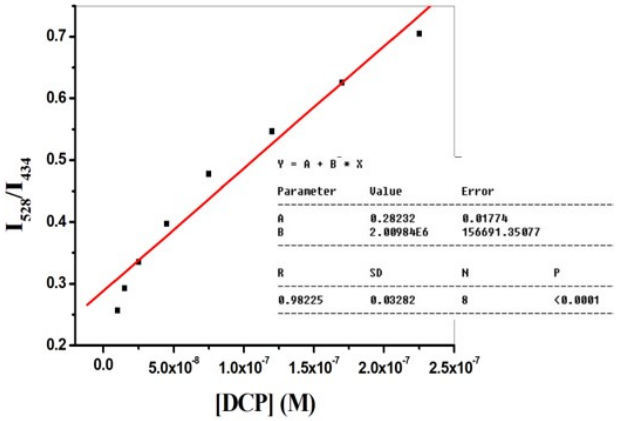

Figure S3. Calibration of the probe at an intensity ratio I_{528}/I_{434} depending on DCP concentration.

LOD= 12.2 nM (R^2=0.98225)

4. pH effect

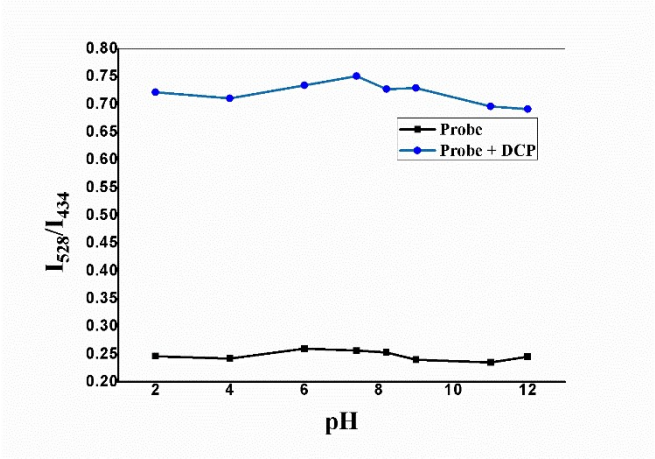

Figure S4. Variation of fluorescence intensity ratio (I_{528}/I_{434}) of MNFZ with the change in pH in ACN/H_2O (9:1 v/v) solution (λ_{ex}=335 nm).

5. Calculation of first order rate constant (k)

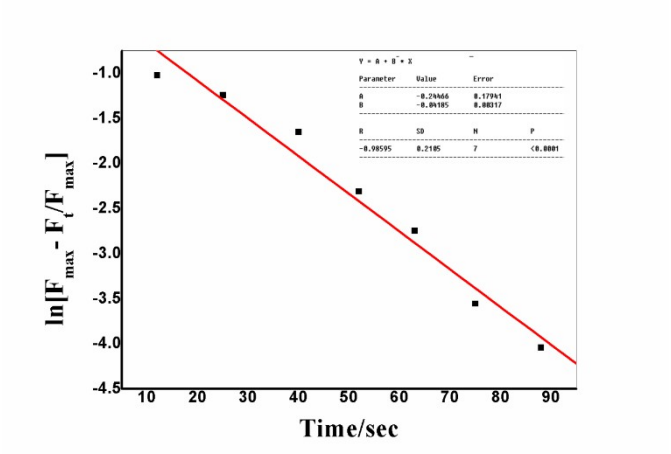

Figure S5. First order kinetic plot of probe (1×10^{-5}M) in the presence of 1×10^{-4}M DCP solution (λ_{ex}=335 nm)

First order rate constant k = 0.04185 s^{-1}

6. Emission spectra of aldehyde (MNPA) and probe (MNFZ)

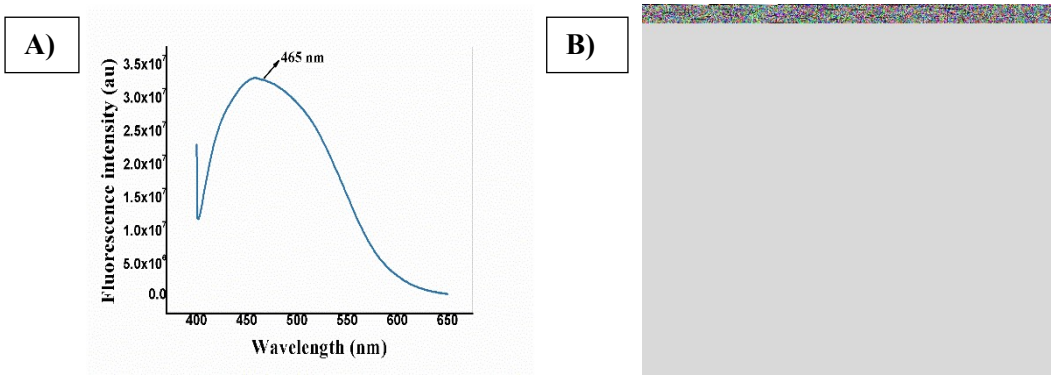

Figure S6. A) Emission spectra of **MNPA** (1×10^{-5}M) in ACN-water (9:1 v/v). **B)** Fluorescence intensity changes of **MNFZ** (1×10^{-5}M) upon gradual addition of DCP in ACN-water (9:1 v/v) (λ_{ex}=335 nm).

7. NMR spectra: ^{1}H-NMR, ^{13}C-NMR

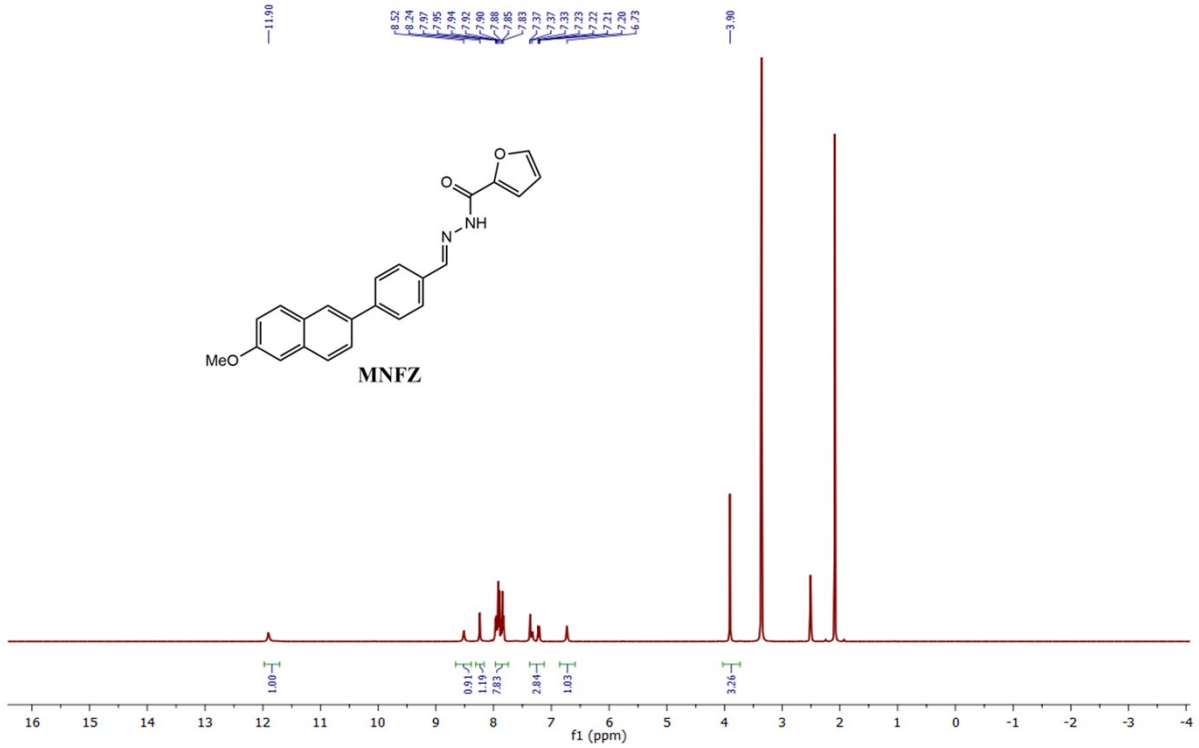

Figure S7: ^{1}H-NMR spectra of MNFZ in DMSO-d_6

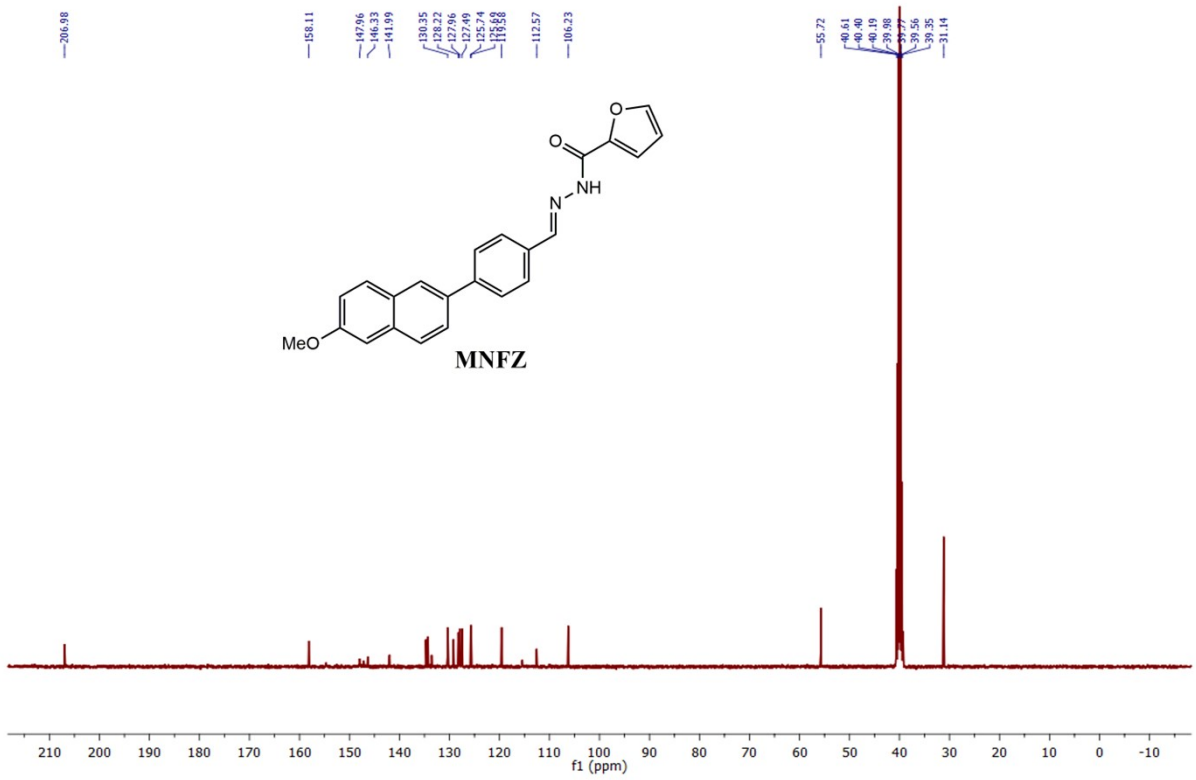

Figure S8 :^{13}C-NMR spectra of MNFZ in DMSO-d_6

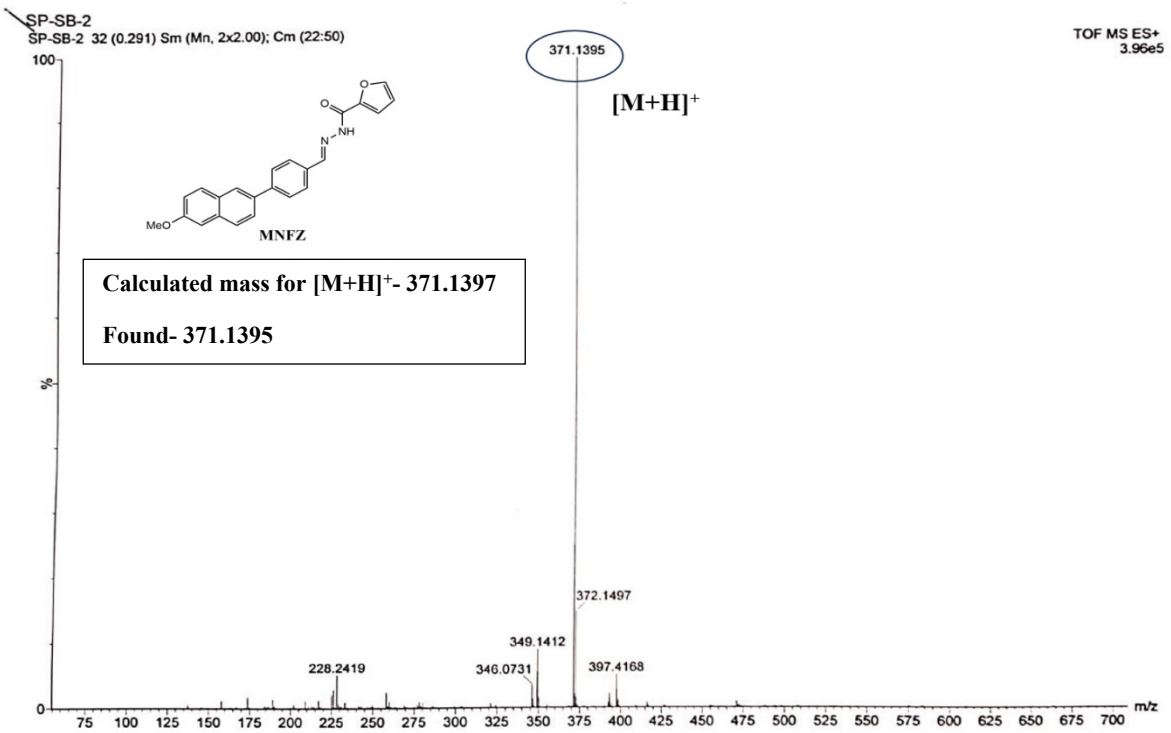

Figure S9: ESI-MS of probe MNFZ

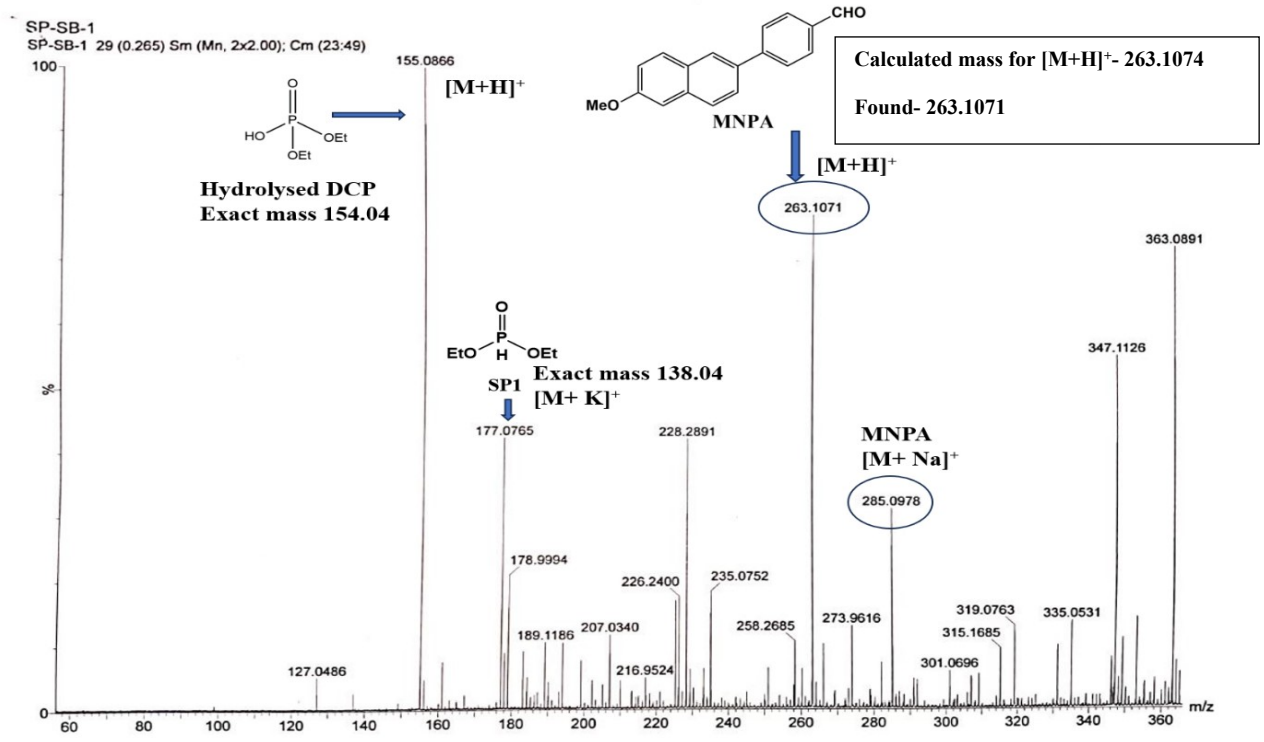

Figure S10: ESI-MS of product MNPA

8. Calculation of fluorescence quantum yield

The fluorescence quantum yield is calculated by the following equation:

$\Phi_x = \Phi_s \times (F_x/F_S) \times (A_s/A_x) \times (\eta_x^2/\eta_s^2)$

Where Φ = quantum yield (Φ_s=0.27)

F_x [3.05×10^9 (MNFZ) and 3.34×10^9 (MNPA)]and F_S (4.45×10^8) are the integrated fluorescence intensity of **MNFZ, MNPA** and fluorescein (reference) respectively.

A_x (0.5 for MNFZ and 0.43 for MNPA) and A_S (0.08) are the absorbance of the **MNFZ, MNPA** and fluorescein (reference) respectively at the excitation wavelength.

η_x (1.34) and η_s (1.36) are the refractive indices of respective solvents employed as Acetonitrile and Ethanol.

So, quantum yield for MNFZ = 0.2874 (28.74 %) and quantum yield for MNPA =0.3660 (36.60%)

9. References:

1. S. S. Ali, A. Gangopadhyay, A. K. Pramanik, U. N. Guria, S. K. Samanta, and A. K. Mahapatra, *Dyes and Pigments*, 2019, **170**, 107585.
2. H. Xu, H. Zhang, L. Zhao, C. Peng, G. Liu, and T. Cheng, *New Journal of Chemistry*, 2020, **44**,10713-10718.
3. K. Aich, S. Das, S. Gharami, L. Patra, and T.K. Mondal, *New Journal of Chemistry*, 2017, **41**,12562-12568.
4. S. Gharami, K. Aich, S. Das, L. Patra, and T.K. Mondal, *New Journal of Chemistry*, 2019, **43**, 8627-8633.
5. S. Zhang, C. Zhou, B. Yang, Y. Zhao, L. Wang, B. Yuan, and H. Li, *New Journal of Chemistry*, 2021, **45**, 7564-7570.
6. D. Li, L. Zong, D. Li, S. Sui, Y. Xiao, B. Zhuang, Y. Shen, Z. Huang, and W. Wu, *Journal of Materials Chemistry C*, 2023, **11**, 4025-4032.
7. M. Mandal, U.N. Guria, S. Halder, A. Karak, D. Banik, K. Jana, A. Kar, and A.K. Mahapatra, *Organic & Biomolecular Chemistry*, 2022, **20**, 4803-4814.
8. A. Karak, S. Banerjee, S. Halder, M. Mandal, D. Banik, A. Maiti, K. Jana, and A.K. Mahapatra, *New Journal of Chemistry*, 2023, **47**, 16756-16763.
9. M. K. Das, T. Mishra, S. Guria, D. Das, J. Sadhukhan, S. Sarker, K. Dutta, A. Adhikary, D. Chattopadhyay, and S.S. Adhikari, *New Journal of Chemistry*, 2023, **47**, 250-257.